

## CHARACTERIZATION OF NEOMYCIN-LOADED XANTHAN-CHITOSAN HYDROGELS FOR TOPICAL APPLICATIONS

IRINA PAULA MERLUSCA,<sup>\*,\*\*,\*\*</sup> CONSTANTA IBANESCU,<sup>\*,\*\*\*\*</sup> CRISTINA TUCHILUS,<sup>\*\*\*\*</sup>  
MARICEL DANU,<sup>\*,\*\*\*\*</sup> LEONARD IONUT ATANASE<sup>\*\*,\*\*</sup> and IONEL MARCEL POPA<sup>\*,\*\*\*\*</sup>

<sup>\*</sup>“Gheorghe Asachi” Technical University of Iasi, Faculty of Chemical Engineering and Environmental Protection, 73, Prof. Dr. Doc. Dimitrie Mangeron Blvd., 700050 Iasi, Romania

<sup>\*\*</sup>Faculty of Dental Medicine, “Apollonia” University, 2, Muzicii Str., Iasi, Romania

<sup>\*\*\*</sup>“Academician Ioan Haulica” Research Institute, 2, Muzicii Str., Iasi, Romania

<sup>\*\*\*\*</sup>“Petru Poni” Institute of Macromolecular Chemistry,  
41 A, Grigore Ghica Voda Alley, 700487 Iasi, Romania

<sup>\*\*\*\*\*</sup>“Grigore T. Popa” University of Medicine and Pharmacy, Faculty of Pharmacy,  
16, University Str., 700115 Iasi, Romania

<sup>\*\*\*\*\*</sup>Academy of Romanian Scientists, 54, Splaiul Independentei, 050094, Bucharest, Romania

✉ Corresponding author: I. P. Merlusca, irinapaulamerlusca@yahoo.com

Received October 30, 2018

Xanthan–chitosan hydrogels are recommended for encapsulation and controlled release of therapeutic agents. Chitosan and neomycin sulphate have been shown to have wound healing properties, when used individually, and a synergetic effect when used together. In this study, drug-loaded xanthan-chitosan hydrogels were prepared with two different neomycin sulphate concentrations, as potential topical formulations. These hydrogels were characterized by rheological studies, thermal analyses, for *in vitro* drug release diffusion, cytotoxicity and antibacterial activity. The results obtained from dynamic rheological experiments demonstrated that the hydrogels behave as weak gels and that their characteristics are strongly influenced by the concentration, pH and temperature. The results provided by thermal analysis suggested that an interaction occurs between xanthan-chitosan and neomycin sulphate. *In vitro* studies demonstrated good retardation of drug release from the hydrogels. Moreover, cell viability studies showed that the hydrogels are non-cytotoxic. Furthermore, the prepared formulations revealed effective bacterial inhibition when exposed to cultures of *Escherichia coli* and *Staphylococcus aureus*.

**Keywords:** xanthan, chitosan, hydrogels, neomycin, rheology, *in vitro* studies

### INTRODUCTION

The skin is one of the largest and most easily accessible organ of the human body and it serves as a route for topical drug administration.<sup>1</sup> Because it interfaces with external environment, the skin plays a key role in protecting the organism against microorganisms, chemicals, ultraviolet radiation, *etc.*, and regulates heat and water loss from the human body.<sup>2-4</sup> The ability of the skin to repair itself in case of minor wounds is remarkable. However, complication appears when the damage is severe or affects large skin areas. In these cases, various kinds of drug-loaded formulations, based on natural and/or synthetic biocompatible polymers, may be applied in order

to protect the wound against infection and pain, and to promote tissue repair.<sup>5,6</sup> Compared to the other delivery routes, topical and transdermal delivery approaches have important advantages, such as direct administration of the drug to the site of the diseased tissues, smaller amounts of drugs are needed to produce a therapeutic effect, plasma level peaking of drugs will be avoided, increased bioavailability due to elimination of hepatic first-pass metabolism, and greatly enhanced patient compliance by eliminating frequent dosing.<sup>7</sup>

Owing to the biocompatibility, biodegradability, antimicrobial and wound

healing activity of chitosan (CS), hydrogels based on CS are frequently used in biomedical and pharmaceutical applications.<sup>8-11</sup> CS is formed by glucosamine and N-acetyl-D-glucosamine monomers in a  $\beta(1\rightarrow4)$  linkage and it is the only cationic polysaccharide.<sup>8,9,12</sup> Therefore, CS is widely used to prepare polyelectrolyte complexes, by electrostatic attractions, with other natural polyanions, such as heparin, xanthan gum, dextran sulfate, carboxymethyl dextran, alginic acid, and carboxymethyl cellulose.<sup>13-16</sup> Among these complexes, an interesting combination is based on CS and xanthan gum (Xa). Xa is a high molecular weight extracellular heteropolysaccharide with a main chain of  $(1\rightarrow4)$ - $\beta$ -D glucose units and side chains of alternating residues of D-mannose and D-glucuronic acid.<sup>17</sup> In combination with other natural-based polymers, xanthan has been applied as excipient in tablets or as supporting hydrogels for drug release applications.<sup>18</sup>

The CS and the Xa molecules present two types of ionizable functional groups: the free carboxyl group of xanthan and the free amino group of chitosan. A hydrogel network is formed by ionic interactions between these groups.<sup>19</sup> During gel formation, even if a large number of the ionizable functional groups are neutralized, a certain amount of ionized groups still remain in the system. Thus, when the gel is dispersed in a chemical, ionic medium, the electrostatic equilibrium will change, due to the ability of the ionized groups to interact with the different ions present in the dispersing medium.<sup>20</sup>

These Xa-CS hydrogels were used for the encapsulation of several drugs, such as theophylline, neomycin, glipizide, metronidazole, and a controlled release of the loaded drugs occurs due to the pH-sensitive swelling behavior of the hydrogels.<sup>21-24</sup> In a recently study of our group, the swelling behavior of neomycin sulphate (Ne) loaded Xa-CS hydrogels in simulated gastric fluid was investigated and *in vivo* studies were performed on healthy Wistar rats.<sup>24</sup> It was demonstrated that the treatment with these Ne-loaded hydrogels improves the biochemical parameters, such as creatinine, urea, serum uric acid and C-reactive protein levels, and prevents histological changes of the colon induced by the toxicity of the free drug.

Ne is an aminoglycoside antibiotic, which is formulated as creams, eye drops or ointments and has been widely used due to its antibacterial

activity.<sup>25,26</sup> Moreover, the combination of neomycin sulphate and chitosan for wound healing has shown synergistic activity, as recently suggested by Gowda *et al.*<sup>25</sup>

The aim of this article was to prepare and investigate Ne-loaded Xa-CS hydrogels, with potential applications in wound healing. The hydrogels were evaluated by rheology and thermogravimetric analyses, *in vitro* Ne release diffusion, cytotoxicity and antimicrobial activity tests.

## EXPERIMENTAL

### Materials

Neomycin sulphate (Ne) was a kind gift sample from Hebei Rongqing Biotechnology Co. Ltd., chitosan (Mw = 94.8 kDa, with a polydispersity index of 3.26 and deacetylation degree of 79.7%) was purchased from Vanson, Inc. (USA), xanthan gum was purchased from Carl Roth (Germany). All the other chemicals and reagents used were of analytical and pharmaceutical grades.

### Synthesis of hydrogels

Xa-CS capsules were prepared by dropwise addition of 2200 mL of Xa solution (0.65% w/v) into 1000 mL of CS solution (0.65% w/v) using a syringe needle (1.1 mm diameter) controlled by a peristaltic pump (flow rate of 1.5 mL/min). The solution was agitated continuously for maturation, for 30 minutes, at room temperature. The hydrogel capsules were filtered, washed with distilled water several times, until a neutral pH was achieved, and then freeze dried for 24 h using a freeze drier (Alpha 1-4 LSC, Christ, Germany). The drug was incorporated into hydrogel matrices through the diffusion process: 1 g of lyophilized capsules was suspended in 10 mL of drug solution (1% w/v). They were gently mixed for 15 minutes for complete diffusion. The resulting complex was lyophilized again. For this study, the drug-loaded hydrogels were prepared using two concentrations of Ne (30% and 50%). The formulations were considered to be 7 wt% dried substance in water or buffer solution at pH 5.5.

### Rheological analysis

Rheological tests were performed on a Physica MCR 501 modular rheometer (Anton Paar, Austria), allowing rheological testing both in controlled stress and control strain modes. Stainless steel parallel-plate serrated geometry, with a diameter of 50 mm, was selected as measuring system. The samples were heated using a Peltier system. All rheological characteristics were determined in the dynamic oscillation mode. For the rheological analyses, all the hydrogels were dispersed, at a concentration of 7 wt%, in both water and buffer solution at pH 5.5, simulating

the pH of the skin surface.<sup>27</sup> Prior to testing, the samples were allowed to rest for at least 300 s. In all the cases, a solvent trap was used to prevent evaporation during measurement.

For rheological characterization of the hydrogel samples, four types of oscillatory tests were performed (amplitude sweep, frequency sweep, time and temperature tests), as well as rotational tests (flow curves). Amplitude sweeps were performed using constant frequency (10 rad/s), while the amplitude was varied between 0.01 and 100%. These tests allowed the determination of the linear viscoelastic (LVE) range for all the samples. Frequency sweep was recorded at constant amplitude in the LVE range and the frequency was varied between 0.1 and 100 rad/s. Oscillatory time tests were carried out at constant amplitude, in the LVE range, and constant frequency. Rotational tests (flow curves) were recorded with a shear rate variation between 0.01 and 100 s<sup>-1</sup>. All these tests were performed at a constant temperature of 25 °C. Temperature tests were performed in the range of 20 °C to 40 °C, with a heating rate of 0.5 °C/min, at constant frequency ( $\omega = 10$  rad/s) and constant amplitude (in the LVE range).

#### Thermo-gravimetric analysis

Thermal properties of the films were investigated by thermo-gravimetric analysis (TGA) on a Mettler Toledo TGA-SDTA 851e, under nitrogen atmosphere, at a 20 mL/min flow rate and a heating rate of 10 °C/min in the range from 25 to 700 °C. The operating parameters were kept constant for all the samples in order to obtain comparable data. The kinetic interpretation was realized with the STARE software offered by Mettler Toledo. To ensure data reproducibility, each analysis was performed in triplicate.

#### In vitro drug release

The following dialysis method was applied: 245 mg of Ne-loaded hydrogel capsules were suspended in 3.5 mL phosphate buffer solution at pH 5.5, sealed in dialysis membrane bags and then immersed in 196.5 mL buffer solution, into vials. The vials were placed in an oscillating water bath at 37±0.5 °C and 50 oscillations/min (SW23, Julabo, Germany). Aliquots of buffer solution (1 mL) were withdrawn at regular intervals of time and replaced immediately with an equal volume of fresh buffer. The Ne concentration was determined using a T60 UV-Vis spectrophotometer (PG Instruments, U.K.) at 570 nm. A standard calibration curve was drawn using Ne as reference. Experiments were performed in triplicate and the average values were taken. The percentage of Ne release was calculated as the ratio between the amount of drug released after 24 h and the amount of drug loaded into capsules.

#### Cytotoxicity

The examination of cytotoxicity was conducted for normal human dermal fibroblasts (NHDF, Lonza). They were cultured in DMEM (Dulbecco's Modified Eagle's Medium – high glucose) containing 10% FBS, supplemented with 1% P/S/N antibiotics and incubated in a humid atmosphere, 5% CO<sub>2</sub> at 37 °C. The fibroblasts were seeded at a density of 1500 cells/well in 96-well plates. The samples were sterilized by UV radiation for 1 h, and the extracts were obtained by incubating the samples in DMEM medium at 37 °C and shaken for 24 hours. After reaching confluence, the cells were treated with medium extract, and re-incubated. The tested extraction solutions were removed and a MTT (Thiazolyl Blue Tetrazolium Bromide) 5% solution was added to each well and then re-incubated for 2.5 hours. The formazan crystals formed in the living cells were dissolved with 200  $\mu$ L isopropanol. The absorbance of formazan was measured at 570 nm using an automatic micro-plate reader (Sunrise, TECAN, Salzburg, Austria). The absorbance value of unexposed cells was taken as control. All experiments were performed in triplicate.

#### Antibacterial activity

The antimicrobial activity was studied using Gram positive bacteria (*Staphylococcus aureus* ATCC 25923), and Gram negative bacteria (*Escherichia coli* ATCC 25922). All these strains were obtained from the Culture Collection of the Department of Microbiology, Faculty of Pharmacy, "Gr. T. Popa" University of Medicine and Pharmacy, Iasi, Romania.

The antimicrobial activity was evaluated by the agar disc diffusion method. A small amount of each microbial culture was diluted in sterile 0.9% NaCl until the turbidity was equivalent to McFarland standard no. 0.5 (10<sup>6</sup> CFU/mL). The suspensions were further diluted 1:10 in Mueller Hinton and then spread on sterile Petri plates (25 mL/Petri plate). Sterile stainless steel cylinders (5 mm internal diameter; 10 mm height) were applied on the agar surface in Petri plates and then 0.1 mL of the tested compounds was added into the cylinders. Commercially available discs containing Ampicillin (25  $\mu$ g/disc), Chloramphenicol (30  $\mu$ g/disc) and Neomycin (30  $\mu$ g/disc) were also placed on the agar surface as positive control. The plates were incubated at 37 °C for 24 h. All the experiments were performed in triplicate; the results were expressed as the diameter of the inhibition zones (mm).

## RESULTS AND DISCUSSION

### Rheological analysis

It is important to study the rheology of Ne-loaded Xa-CS hydrogels for understanding the effect of the dispersing media, hydrogel composition and the encapsulation of the Ne drug on the structure, mechanical properties, and

storage stability of the hydrogels. Moreover, the rheological properties of these hydrogels are extremely important in predicting and evaluating their consistency, texture, sensory properties and acceptability by the patient.<sup>28,29</sup>

The presence of a weak gel network with a semi-flexible structure was evidenced for xanthan molecules in aqueous solution due to the intermolecular interactions (hydrogen bonding, electrostatic and hydrophobic interactions). The rheological properties of xanthan solutions are significantly influenced by modifications of the physical interactions in system. Under stress, the physical bonds in the gel network can be easily broken down, allowing the system to flow and thus inducing the shear-thinning behavior. On the other hand, even at low concentrations, chitosan molecules are linked by strong intermolecular hydrogen bonds, thus exhibiting high ability to entangle and form a network. A wide range of parameters influence the rheological properties of chitosan-based hydrogels: pH, ionic strength, solvent, concentration, molecular weight, and the distribution of the acetyl groups.<sup>30</sup> By increasing the pH of the solution, the hydrodynamic volume of the chitosan molecules decreases because of the reduction in the electrostatic repulsions

between cationic charges, allowing the chains to come closer and thus increasing the number of the inter- and intra-chain hydrogen bonds.<sup>20,30</sup>

Typical flow curves at 25 °C were recorded both for Xa-CS and Xa-CS-Ne hydrogels. Figure 1 illustrates the variation of the dynamic viscosity with shear rate, both in water and buffer solution as dispersion media.

For all the systems, the close proximity of the neighboring chains constrained the movement of the entangled chains and, when the shear rate was increased, a decrease in viscosity was noticed, probably caused by the disentanglement of the polymer chains due to the reptation process. Moreover, a Newtonian region in the low shear rate characterized by constant viscosity ( $\eta_0$  – zero-shear viscosity) could be observed for all the hydrogels. This behavior can be explained by the well-established balance between the disruptions of the entanglements induced by the shear rate and the formation of new ones. The values of the zero-shear rate viscosity were influenced by the nature of the dispersion medium and the Ne content of the samples (Table 1).

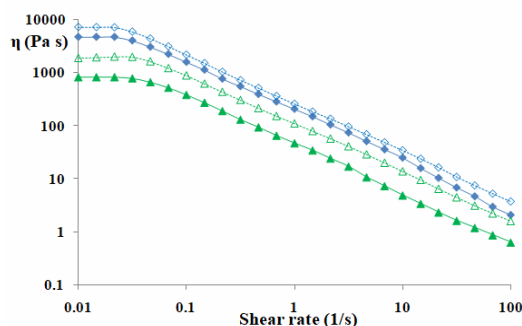


Figure 1: Flow curves for Xa-CS hydrogel samples in water (full diamonds) and buffer solution (open diamonds) and for Xa-CS-Ne 50% hydrogel samples in water (full triangles) and buffer solution (open triangles)

Table 1  
Zero shear viscosity values of the hydrogels (Carreau-Yasuda model)

Sample	$\eta_0$ (Pa s)	
	Water	Buffer solution
Xa-CS	31665	7479
Xa-CS-Ne 30%	2583	3654
Xa-CS-Ne 50%	898	2032

At higher shear rates, the disruption of entanglements predominates over the formation of new ones as most molecules are aligned in the flow direction, therefore the dynamic viscosity decreased with increasing the shear rate. A non-Newtonian shear-thinning behavior was obvious for all the analyzed hydrogels, both in water and buffer solution, at shear rates higher than  $0.03 \text{ s}^{-1}$ . At high shear rates, the hydrogels dispersed in water are characterized by lower resistance to flow, because of the decrease in the physical interaction between the macromolecular chains. Moreover, the encapsulation of increasing amounts of Ne in these hydrogels can cause the disruption of the hydrogel structure, leading to lower viscosities. Therefore, as the Ne content in the system increased, the re-organization of the inter-molecular and/or intra-molecular interactions seems to have occurred.

Oscillatory tests (amplitude, frequency, time and temperature sweeps) were performed in order to better estimate the rheological behavior of the prepared Xa-CS hydrogels in the presence and in the absence of Ne. The amplitude sweep allowed establishing the limits of the linear viscoelastic (LVE) range, as well as the structural and mechanical stability of the hydrogels. For this purpose, stress sweep tests at a frequency of 10 rad/s were carried out. For all the studied hydrogels, stable structures were evidenced for a wide range of deformations, as illustrated in Figure 2. Higher dynamic moduli values and extended LVE range limits were noticed for the hydrogels dispersed in the buffer solution at pH 5.5 (Fig. 2b) vs water (Fig. 2a), which can be explained by the ionic nature of the systems. Moreover, both in water and in the buffer solution, the addition of Ne decreased both the storage ( $G'$ ) and the loss ( $G''$ ) moduli, but it had an insignificant effect on the gel structure stability. The limits of the LVE region were determined, for all the analyzed hydrogels, in terms of both deformation (0.5-5%) and stress (1-19 Pa).

In the frequency sweep test, as illustrated in Figure 2, the storage modulus ( $G'$ ), the loss modulus ( $G''$ ) and complex viscosity ( $|\eta^*|$ ) were recorded when a sinusoidal strain was applied at a constant amplitude within the LVE region. The

oscillation frequency was varied between  $10^{-1}$  and  $10^2$  rad/s. The mechanical spectra of the hydrogels allow clear differentiation between weak and strong gels.<sup>18</sup> Usually, the dynamic moduli of strong gels are independent of frequency for more than three decades, an obvious indication of covalent bonds occurrence, while pronounced dependence on frequency is characteristic of physical, weak gels. As expected, a weak gel structure was noticed for all the Xa-CS and Ne-loaded Xa-CS hydrogels, with  $G' > G''$  for the entire experimental domain. Moreover, an obvious dependence of the two dynamic moduli on frequency was observed.

For experiments carried out in the LVE range at  $\omega = 0.1$  rad/s, where the  $G' > G''$ , three particular cases were previously established:<sup>31</sup> (i) if  $G' \geq 10$  Pa, a certain dispersion stability or gel stability can be assumed; (ii) if  $G' \leq 1$  Pa, the stability related to practical use is hardly present, and (iii) if  $1 \leq G' \leq 10$ , further tests should be carried out (*e.g.* yield stress and flow point). For all the studied samples,  $G'$  at  $\omega = 0.1$  rad/s is much higher than 10 Pa, suggesting very good structure stability in both dispersion media. Moreover, the values of the dynamic moduli were higher for the hydrogels dispersed in buffer solution (Fig. 3b), while the influence of the added Ne was more pronounced for water as dispersion medium (higher difference between the moduli) (Fig. 3a). The increase in the Ne content leads to a decrease of the hydrogel strength ( $G'$ ), the gels were softer, but still with a very stable structure. The variation in the elasticity of the hydrogels may arise from a diminution of the interaction number and entanglements among the polysaccharide chains, caused by the presence of Ne.

The dependence of complex viscosity on frequency (Table 2) for all the analyzed hydrogels revealed the pseudoplastic behavior (shear thinning behavior), which is a requirement for pharmaceutical gels designed for topical applications.<sup>28</sup> As observed from Table 2, the complex viscosity values decrease with increasing frequency, for all the types of hydrogels. Moreover, at equal frequency, the immobilization of Ne leads to a decrease of the complex viscosity values.

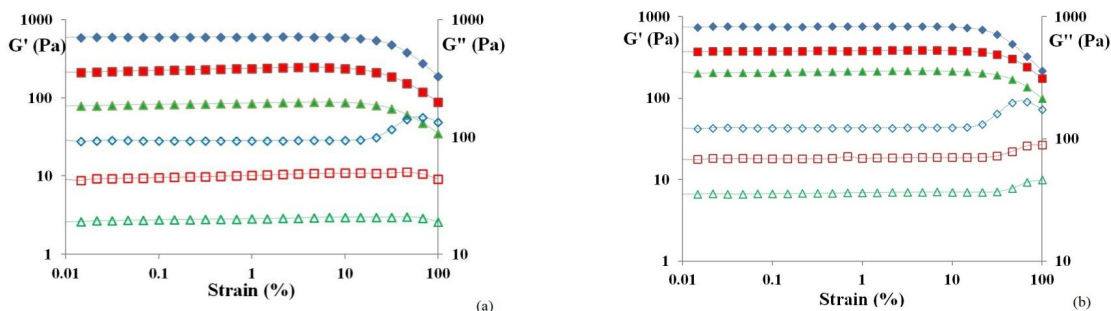


Figure 2: Amplitude sweep tests for hydrogels in water (a) and buffer solution (b): full and open diamonds for  $G'$  and  $G''$  (Xa-CS), full and open squares for  $G'$  and  $G''$  (Xa-CS-Ne 30%), full and open triangles for  $G'$  and  $G''$  (Xa-CS-Ne 50%)

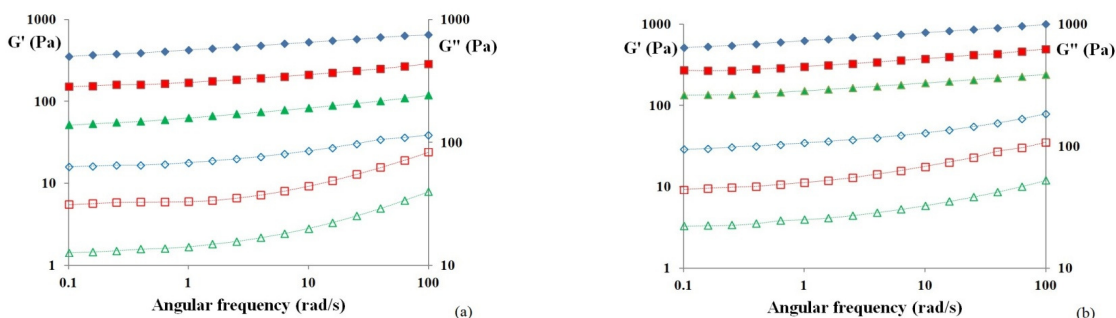


Figure 3: Frequency tests for hydrogel samples in water (a) and buffer solution (b): full and open diamonds for  $G'$  and  $G''$  (Xa-CS), full and open squares for  $G'$  and  $G''$  (Xa-CS-Ne 30%), full and open triangles for  $G'$  and  $G''$  (Xa-CS-Ne 50%)

Oscillatory time sweep tests, given in Figure 4 for sample Xa-CS-Ne 50% in water and buffer solution as a typical example, were performed at constant frequency ( $\omega = 10$  rad/s) and constant amplitude (within LVE range) in order to estimate the structural stability and integrity of the prepared hydrogels.

These tests revealed that the hydrogels are stable in time both in water and in buffer solution, as illustrated in Figure 4. Moreover, the same influence of the dispersion medium was observed as in previous rheological tests: dynamic moduli and thus, the strength of the gels, are slightly increased for the systems dispersed in the buffer solution at pH 5.5. By encapsulation of Ne, the gel networks became softer and smoother, being thus adequate candidates for topical applications. For some systems, a slight increase in the dynamic moduli over time was observed, which can be explained by the relaxation effect and possible evaporation effects leading to hydrogel concentration.

Dynamic temperature sweep tests were performed after equilibration at the initial temperature (20 °C) and the evolution of the elastic and viscous moduli as a function of temperature is presented in Table 3.

For the hydrogels dispersed in water, an increase in  $G'$  (gel strength) with more than two orders of magnitude was noticed when the temperature exceeded 25 °C (Table 3). The gel structure was not disturbed, but the detachment of surrounding water molecules could be assumed to occur, thus allowing the association of the hydrophobic segments of Xa and CS.<sup>32</sup> This effect was shifted to higher temperatures in the case of the hydrogels dispersed in buffer solutions, proving once more the effect of the ionic dispersion media on the gel properties. The encapsulation of the drug led to the softening of the gels dispersed in water, whereas the opposite effect was observed at higher temperatures for the hydrogels dispersed in the buffer solution, probably because of the effect of stronger electrostatic interactions.

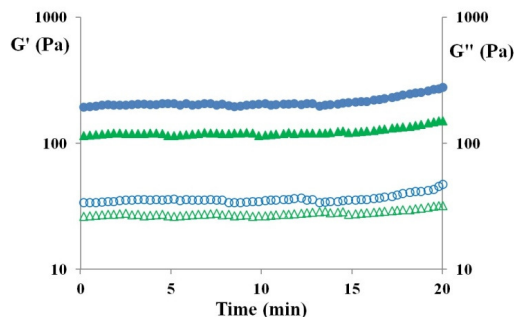


Figure 4: Oscillatory time test for Xa-CS-Ne 50% hydrogel sample in water (circles) and buffer solution (triangles):  $G'$  (full circles and triangles) and  $G''$  (open circles and triangles)

Table 2  
Frequency dependence of complex viscosity ( $\eta^*$ ) for hydrogel samples in water and buffer solution

$\omega$ (Pa s)	$\eta^*$					
	Water			Buffer solution		
	Xa-CS	Xa-CS-Ne 30%	Xa-CS-Ne 50%	Xa-CS	Xa-CS-Ne 30%	Xa-CS-Ne 50%
0.1	4220	1880	585	5260	2770	1430
1	429	174	64	633	305	153
10	53	22	9	80	38	19
100	7	3	1	10	5	2

Table 3  
Temperature dependence of dynamic moduli  $G'$  and  $G''$  for hydrogel samples in water and buffer solution

T (°C)	$G'$ (Pa)						$G''$ (Pa)					
	Water			Buffer solution			Water			Buffer solution		
	Ne 0%	Ne 30%	Ne 50%	Ne 0%	Ne 30%	Ne 50%	Ne 0%	Ne 30%	Ne 50%	Ne 0%	Ne 30%	Ne 50%
20	668	375	215	755	349	115	114	60	45	122	67	40
25	798	458	252	735	413	140	127	70	50	124	71	51
30	2570	1490	458	770	663	346	365	220	136	132	102	89
35	10800	6670	2900	1560	7720	1840	1190	810	696	1236	959	496
40	72500	31300	18800	40300	37900	12500	9850	3180	2980	4710	3410	1280

### Thermo-gravimetric analysis

The thermo-gravimetric analysis applied to the hydrogels, to the drug, as well as to the drug-loaded hydrogels offers information on the manner in which thermal decomposition takes place in an inert environment. The decomposition of the Xa-CS hydrogels occurs in two stages, while that of the drug and of the drug-loaded hydrogels occurs in three stages, as shown in Figure 5.

As illustrated in Figure 5, the peak characteristic of the second stage of the Ne degradation, occurring around 235 °C, also occurs in the case of the Xa-CS-Ne hydrogels. The intensity of the peak increases, by increasing the amount of the loaded Ne, which confirms the drug's immobilization within the hydrogel network.

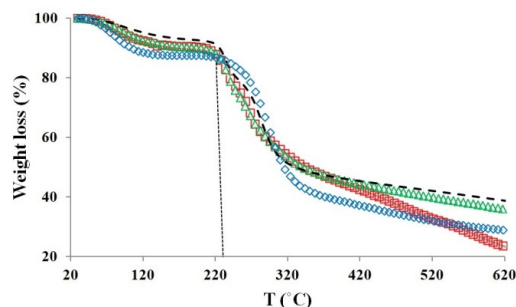


Figure 5: TGA curves of Xa-CS (diamonds), Xa-CS-Ne 30% (squares), Xa-CS-Ne 50% (triangles) and Ne (dotted line)

### ***In vitro* drug release**

The partition coefficient of the drug between the polymeric phase and the aqueous environment, as well as the diffusion of the drug across the dialysis membrane are the driving forces for the release rate of the drug from the hydrogel networks. The dialysis membrane bags retained the hydrogel capsules and allow the free diffusion of the Ne immediately into the release media. *In vitro* release profiles of the Ne are provided in Figure 6.

The Xa-CS hydrogels showed a fast initial drug release during the first 12 h, followed by a

slower and continuous sustained release over 24 h. The initial burst of drug was attributed to surface associated drug, and the slower release phase was due the drug entrapped in the hydrogel network. The cumulative percentage drug release from the drug-loaded hydrogels was found to be of 70%, for the Xa-CS-Ne 30%, and of 84% for the Xa-CS hydrogels loaded with 50% Ne, respectively (Fig. 6). Moreover, the drug release efficiency was found to reach the maximum level after 24 h for all the analyzed samples.

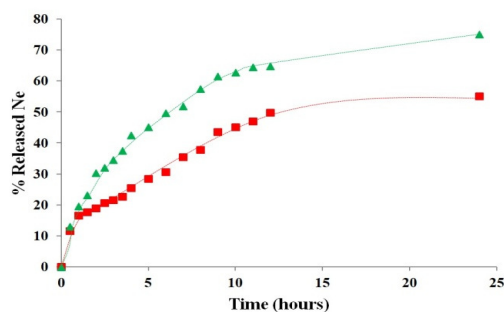


Figure 6: *In vitro* release profiles of Ne from Xa-CS hydrogels in phosphate buffer solution (pH 5.5) at 37 °C: Xa-CS-Ne 30% (squares) and Xa-CS-Ne 50% (triangles)

### **Cytotoxicity**

The assessment of cytotoxicity is an important part of the drug-loaded hydrogels evaluation, as these materials would be in direct contact with living cells during their application.<sup>12</sup> Figure 7 shows the cell viability at regular time intervals (24, 48 and 72 hours) of different species at a concentration of 0.1 mg.mL<sup>-1</sup>.

As illustrated in Figure 7, cell viability was higher than 80% for all the analyzed samples, therefore Ne-loaded Xa-CS hydrogels can be reported as

safe for biomedical applications. In fact, as recommended by Bombaldi de Souza *et al.*,<sup>33</sup> the Xa-CS membranes are recommended for moderately to highly exuding wounds. At high Ne concentrations, cell viability decreases. Chellat *et al.*,<sup>17</sup> which evaluated the biocompatibility of the xanthan-chitosan microspheres, found that Xa-CS particles showed significant growth inhibition, when they were used at concentrations of 5 and 10 mg.mL<sup>-1</sup>.



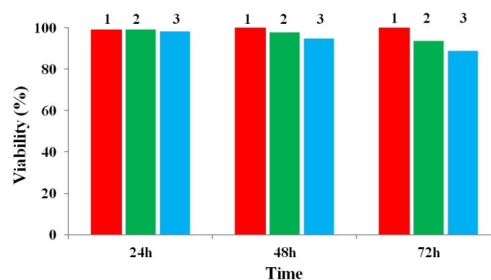


Figure 7: Percentage cell viability in NHDF cells, at different time intervals: (1) Xa-CS, (2) Xa-CS-Ne 30%, (3) Xa-CS-Ne 50%

### Antibacterial activity

Table 4 presents the results concerning the antimicrobial effects of the Xa-CS hydrogels loaded with 50% Ne. As observed in Table 4, all the samples were effective against *Escherichia coli* and *Staphylococcus aureus* strains. The highest inhibition zone was observed for the Ne powder solution, which can be the consequence of the fact that the drug was not completely released after 24 h. Moreover, it appears that, despite the important antimicrobial role of the chitosan, the Ne-loaded Xa-CS hydrogels developed larger

zones of inhibition than the drug-free Xa-CS hydrogels. The antimicrobial effect of chitosan is due to its cationic nature. The interaction between the amino groups of chitosan with the anionic components of microorganisms (lipopolysaccharides, teichoic acid) is assumed to be the main antimicrobial mechanism.<sup>34</sup> Regarding the efficiency against bacteria, all the samples showed inferior activity against *Escherichia coli* by comparison with that against *Staphylococcus aureus*, which was more pronounced.

Table 4  
Antimicrobial effects of Xa-CS-Ne 50%

Extract/positive control	Diameter of inhibition area (mm)	
	<i>Staphylococcus aureus</i> ATCC 25923	<i>Escherichia coli</i> ATCC 25922
Ne <sup>a</sup>	26±0.5	24±0.6
Xa-CS <sup>a</sup>	18±0.6	13±1.0
Xa-CS-Ne 50% <sup>b</sup>	23±0.6	21±0.5
Ampicillin <sup>c</sup>	30±0.6	19±0.5
Chloramphenicol <sup>d</sup>	29±0.1	30±0.6
Neomycin <sup>d</sup>	21±1.0	21±0.5

<sup>a</sup> 20 µg/well; <sup>b</sup> 40 µg/well; <sup>c</sup> 25 µg/disc; <sup>d</sup> 30 µg/disc

### CONCLUSION

The aim of our study was to prepare and characterize Ne-loaded Xa-CS hydrogels with a view to their use for topical applications. These hydrogels have been rheologically characterized by rotational and oscillatory shear measurements. The analyzed samples exhibited stable structure, characteristic of physical weak gels, with frequency dependent dynamic moduli, and  $G'$  higher than  $G''$  for the entire experimental domain. The influence of the dispersion media, Ne content and temperature, on the hydrogel structure was also studied. Higher moduli were obtained for the hydrogels dispersed in buffer solution, as compared to those dispersed in water,

due to the increased ionic strength, which modifies the internal structure of the hydrogel network. Increasing the Ne content leads to a decrease of the dynamic moduli values, producing smooth, soft, easily spreadable gels, which can be suitable for applications in creams and ointments for wound healing. For all the samples, a shear-thinning behavior was observed, which is a prerequisite condition for biomedical applications. The final structure and the final properties of these hydrogels were strongly influenced by a series of factors, such as hydrogel composition, Ne content, dispersion medium and temperature. The interactions among these factors must be considered in order to prepare hydrogels with

desired properties for topical applications. The results provided by thermal analysis confirmed the immobilization of Ne in the hydrogel network. *In vitro* release studies revealed that the hydrogels can sustain the release of Ne for about 24 hours. The drug remains localized for a longer period of time, thus enabling drug targeting to the skin and feasibility of use. Then, the antimicrobial test confirmed that the formulations offered prolonged drug release. The prepared formulations demonstrated effective bacterial inhibition when exposed to cultures of *Escherichia coli* and *Staphylococcus aureus*. The non-toxicity of these Ne-loaded Xa-CS hydrogels validates them as potential drug delivery systems.

**ACKNOWLEDGEMENTS:** The research works have been supported by a grant of the Romanian National Authority for Scientific Research, CNCS-UEFISCDI, project number PN-III-P2-2.1-BG-2016-0175.

## REFERENCES

- <sup>1</sup> P. O. Nnamani, E. U. Dibua, F. C. Kenechukwu, C. C. Ogbonna, C. Onyemaechi *et al.*, *Afr. J. Biotechnol.*, **14**, 979 (2015), <https://doi.org/5897/AJB2013.12976>
- <sup>2</sup> N. Tabassum and M. Hamdani, *Pharmacogn. Rev.*, **8**, 52 (2014), <https://doi.org/10.4103/0973-7847.125531>
- <sup>3</sup> O. Uchechi, J. D. N. Ogbonna and A. A. Attama, in "Application of Nanotechnology in Drug Delivery", edited by A. D. Sezer, InTech, Rijeka, 2014, pp. 193-235, <http://dx.doi.org/10.5772/58672>
- <sup>4</sup> A. Z. Alkilani, M. T. C. McCrudden and R. F. Donnelly, *Pharmaceutics*, **7**, 438 (2015), <https://doi.org/10.3390/pharmaceutics7040438>
- <sup>5</sup> S. M. Lee, I. K. Park, Y. S. Kim, H. J. Kim, H. Moon *et al.*, *Biomater. Res.*, **20**, (2016), <https://doi.org/10.1186/s40824-016-0063-5>
- <sup>6</sup> T. V. L. Hima Bindu, M. Vidyavathi, K. Kavitha, T. P. Sastry and R. V. Suresh Kumar, *Trends Biomater. Artif. Organs*, **24**, 123 (2010), <http://www.sbaio.org/tibao/>
- <sup>7</sup> H. Marwat, T. Garg, A. K. Goyal and G. Rath, *Drug Deliv.*, **23**, 564 (2016), <https://doi.org/10.3109/10717544.2014.935532>
- <sup>8</sup> J. P. Menda, T. Reddy, R. Deepika, M. Pandima Devi and T. P. Sastry, *Am. J. Phyromed. Clin. Ther.*, **2**, 61 (2014), <http://www.imedpub.com/articles/preparation-and-characterization-of-woundhealing-composites-of-chitosan-aloe-veraand-calendula-officinalis--a-comparativestudy.pdf>
- <sup>9</sup> E. Sipos, N. Szász, S. Vancea and A. Ciurba, *Trop. J. Pharm. Res.*, **13**, 1987 (2014), <https://doi.org/10.4314/tjpr.v13i12.5>
- <sup>10</sup> A. Salama, *Cellulose Chem. Technol.*, **52**, 903 (2018), [http://www.cellulosechemtechnol.ro/pdf/CCT9-10\(2018\)/p.903-907.pdf](http://www.cellulosechemtechnol.ro/pdf/CCT9-10(2018)/p.903-907.pdf)
- <sup>11</sup> F. Akman, *Cellulose Chem. Technol.*, **51**, 253 (2017), [http://www.cellulosechemtechnol.ro/pdf/CCT3-4\(2017\)/p.253-262.pdf](http://www.cellulosechemtechnol.ro/pdf/CCT3-4(2017)/p.253-262.pdf)
- <sup>12</sup> M. Z. Bellini, P. Oliva-Neto and A. M. Moraes, *Braz. Arch. Biol. Technol.*, **58**, 289 (2015), <http://dx.doi.org/10.1590/S1516-8913201500305>
- <sup>13</sup> A. Borzacchiello, L. Ambrosio, P. A. Netti, L. Nicolais, C. Peniche *et al.*, *J. Mater. Sci.: Mater. Med.*, **12**, 861 (2001), <https://doi.org/10.1023/A:1012851402759>
- <sup>14</sup> F. Ahmadi, Z. Oveisi, S. M. Samani and Z. Amoozgar, *Res. Pharm. Sci.*, **10**, 1 (2015), <https://www.ncbi.nlm.nih.gov/pmc/articles/PMC4578208/>
- <sup>15</sup> X. Huang, R. Wang, T. Lu, D. Zhou, W. Zhao *et al.*, *Biomacromolecules*, **17**, 3883 (2016), <https://doi.org/10.1021/acs.biomac.6b00956>
- <sup>16</sup> L. Racine, I. Texier and R. Auzely-Velty, *Polym. Int.*, **66**, 981 (2017), <https://doi.org/10.1002/pi.5331>
- <sup>17</sup> F. Chellat, M. Tabrizian, S. Dumitriu, E. Chornet, P. Magny *et al.*, *J. Biomed. Mater. Res.*, **51**, 107 (2000), [https://doi.org/10.1002/\(SICI\)1097-4636\(200007\)51:1<107::AID-JBM14>3.0.CO;2-F](https://doi.org/10.1002/(SICI)1097-4636(200007)51:1<107::AID-JBM14>3.0.CO;2-F)
- <sup>18</sup> D. F. S. Petri, *J. Appl. Polym. Sci.*, **132**, 42035 (2015), <https://doi.org/10.1002/app.42035>
- <sup>19</sup> S. Argin-Soysal, P. Kofinas and Y. M. Lo, *Food Hydrocoll.*, **23**, 202 (2009), <https://doi.org/10.1016/j.foodhyd.2007.12.011>
- <sup>20</sup> A. Martinez-Ruvalcaba, E. Chornet and D. Rodrigue, *Carbohydr. Polym.*, **67**, 586 (2007), <https://doi.org/10.1016/j.carbpol.2006.06.033>
- <sup>21</sup> A. F. Eftaiha, N. Qinna, I. S. Rashid, M. M. Al Remawi, M. R. Al Shami *et al.*, *Mar. Drugs*, **8**, 1716 (2010), <https://doi.org/10.3390/md8051716>
- <sup>22</sup> N. Kulkarni, P. Wakte and J. Naik, *Int. J. Pharm. Investig.*, **5**, 73 (2015), <http://dx.doi.org/10.4103/2230-973X.153381>
- <sup>23</sup> N. Popa, O. Novac, L. Profire, C. E. Lupusoru and M. I. Popa, *J. Mater. Sci.: Mater. Med.*, **21**, 1241 (2010), <https://doi.org/10.1007/s10856-009-3937-4>
- <sup>24</sup> I. P. Merlusca, P. Plamadeala, C. Girbea and I. M. Popa, *Cellulose Chem. Technol.*, **50**, 577 (2016), [www.cellulosechemtechnol.ro/pdf/CCT5-6\(2016\)/p.577-583.pdf](http://www.cellulosechemtechnol.ro/pdf/CCT5-6(2016)/p.577-583.pdf)
- <sup>25</sup> D. V. Gowda, M. P. Gowrav, A. Srivastava and R. A. M. Osmani, *Der Pharma. Lett.*, **8**, 128 (2016), <https://www.scholarsresearchlibrary.com/articles/a-study-of-chitosan-nanofibers-containing-neomycin-sulphate-for-wound-healing-activity.pdf>

- <sup>26</sup> T. Nitanan, P. Akkaramongkolporn, T. Rojanarata, T. Ngawhirunpat and P. Opanasopit, *Int. J. Pharm.*, **448**, 71 (2013), <https://doi.org/10.1016/j.ijpharm.2013.03.011>
- <sup>27</sup> N. A. El-Gendy, G. A. Abdelbary, M. H. El-Komy and A. E. Saafan, *Curr. Drug Deliv.*, **6**, 50 (2009), <https://doi.org/10.2174/156720109787048276>
- <sup>28</sup> C. A. Gafițanu, D. Filip, C. Cernătescu, C. Ibănescu, M. Danu *et al.*, *Biomed. Pharmacother.*, **83**, 485 (2016), <https://doi.org/10.1016/j.biopha.2016.06.053>
- <sup>29</sup> J. Hurler, A. Engesland, B. P. Kermany and N. Skalko-Basnet, *J. Appl. Polym. Sci.*, **125**, 180 (2012), <https://doi.org/10.1002/app.35414>
- <sup>30</sup> A. Venault, L. Vachoud, D. Bouyer, C. Pochat-Bohatier and C. Faur, *J. Appl. Polym. Sci.*, **120**, 808 (2011), <https://doi.org/10.1002/app.33105>
- <sup>31</sup> C. Ibănescu, M. Danu, A. Nanu, M. Lungu and B. C. Simionescu, *Rev. Roum. Chim.*, **55**, 933 (2010), [http://revroum.lew.ro/wp-content/uploads/2010/RRCh\\_11-12\\_2010/Art%2022.pdf](http://revroum.lew.ro/wp-content/uploads/2010/RRCh_11-12_2010/Art%2022.pdf)
- <sup>32</sup> A. R. Taherian, P. Lacasse, B. Bisakowski, M. Pelletier, S. Lanctot *et al.*, *Food Hydrocoll.*, **63**, 635 (2017), <https://doi.org/10.1016/j.foodhyd.2016.09.031>
- <sup>33</sup> R. F. Bombaldi de Souza, F. C. Bombaldi de Souza and A. M. Moraes, *J. Appl. Polym. Sci.*, **134**, 45386 (2017), <https://doi.org/10.1002/app.45386>
- <sup>34</sup> E. Malinowska-Pańczyk, H. Staroszczyk, K. Gottfried, I. Kolodziejska and A. Wojtasz-Pajak, *Polimery*, **60**, 735 (2015), <https://dx.doi.org/10.14314/polimery.2015.735>